

## **On the Shear-Deformation Theories for the Analysis of Concrete Shells Reinforced with External Composite Laminates**

**A. J. M. Ferreira**

Departamento de Engenharia Mecânica e Gestão Industrial Faculdade de Engenharia da Universidade do Porto, Porto, Portugal

## **Применение различных теорий сдвиговой деформации для расчета бетонных оболочек, армированных внешними композитными ламинатами**

**А. Ж. М. Феррейра**

Университет г. Порто, Португалия

*Предложена теория сдвиговой деформации третьего порядка для описания напряженно-деформированного состояния бетонных оболочек, армированных внешними композитными ламинатами. Армированные бетонные конструкции – главные компоненты в строительной отрасли. Коррозия стальных балок, используемых для армирования железобетонных конструкций, является очень актуальной проблемой, которая усугубляется за счет пористости бетона. В качестве адекватного решения проблемы упрочнения и модификации ослабленных конструкций практикуется использование внешних композитных ламинатов, которые закрепляются на наружных поверхностях бетонных конструкций. Деформирование такого рода конструкций характеризуется значительной нелинейностью. Для разработки нелинейных геометрических моделей и моделей материала используются численные методы, в частности метод конечных элементов. Для анализа композитных ламинатов все чаще используются сдвиговые деформации высокого порядка. Предлагаемая теория является альтернативой теории первого порядка, ранее предложенной Феррейра с соавторами. Теория опробована на элементе оболочки, структура которого позволяет воспроизвести послойную дискретизацию ламинатных материалов. Для моделирования деформирования бетона при сжатии использовались подходы идеально пластического и пластически-упрочняемого поведения материала. Рассмотрен двойственный критерий течения и разрушения материала с точки зрения напряжений и деформаций, который применяется в сочетании с представлением деформационной кривой при растяжении в виде ломаной линии с горизонтальным участком, соответствующим началу пластического течения. Однонаправленные композитные полосы характеризуются линейно-упругим (хрупким) поведением. Выполнен конечно-элементный расчет напряженно-деформированного состояния армированной композитными полосами бетонной балки, подвергнутой трехточечному изгибу. Описаны наблюдаемые эффекты армирования, результаты применения теории третьего порядка и дан сравнительный анализ упрочнения бетонной конструкции композитными полосами и стальной арматурой.*

**Ключевые слова:** бетонная оболочка, конечно-элементный анализ, армирование волокнитом, композитный материал, комбинированное армирование, трехмерная теория.

**Introduction.** Reinforced concrete (RC) structures are very important in civil construction industry.

For many years, the structural analysis of RC was based on empirical laws and elasticity equations. Concrete is a complex material with cracking, tension stiffening, plasticity, and nonlinear properties. Numerical methods such as the finite element method are needed for such an analysis [1–3].

Corrosion of steel re-bars is a common problem due to the porosity of concrete. The use of external composites (FRP) bonded to the faces of concrete are today a good solution to retrofitting of degraded structures [4–6]. The need for numerical methods is even greater than with conventional reinforced concrete.

The use of higher-order shear deformations is now common in the analysis of composite laminates [7–10].

In this paper, it is intended to study the behavior of reinforced concrete strengthened with thin unidirectional composite strips mainly on the tension side by the use of the finite element method.

The nonlinear material model for concrete and for composite strips is applied to a shell element. The geometrical and material nonlinear behavior is accounted for [11–13]. Some results are discussed.

**Compressive Behavior of Concrete.** The nonlinear behavior of concrete is inelastic. A perfect plastic and a strain-hardening plasticity approaches are used to model the compressive behavior of concrete. A dual criterion for yielding and crushing in terms of stresses and strains is considered, which is complemented by a tension cut-off representation.

*The Yield Condition.* The yield condition for thick plates and shells accounting for transverse shear effects is formulated in terms of the first two stress invariants as

$$f(I_1, J_2) = [\beta(3J_2) + \alpha I_1]^{1/2} = \sigma_0, \quad (1)$$

where  $\alpha$  and  $\beta$  are material parameters and  $\sigma_0$  is the effective stress obtained from a uniaxial compression test. Relating this expression to Kupfer's results [14], the material parameters are

$$\alpha = 0.355\sigma_0 \quad \text{and} \quad \beta = 1.355. \quad (2)$$

In the perfectly plastic model,  $\sigma_0$  is taken as the ultimate stress  $f'_c$  obtained from a uniaxial compressive test. An elastic response is assumed up to when the effective stress reaches  $f'_c$ , after which a perfectly plastic response follows until the limiting surface is reached. Figure 1 illustrates a one-dimensional representation of both the perfectly plastic and the strain-hardening models [11, 12].

*The Crushing Condition.* The crushing condition is a strain-controlled phenomenon. The lack of experimental information necessitates a direct conversion of (1) into strains. Thus,

$$[\beta(3J'_2) + \alpha I'_1]^{1/2} = \varepsilon_u^2, \quad (3)$$

where  $I'_1$  and  $J'_2$  are strain invariants and  $\varepsilon_u$  is the ultimate total strain extrapolated from the uniaxial test results.

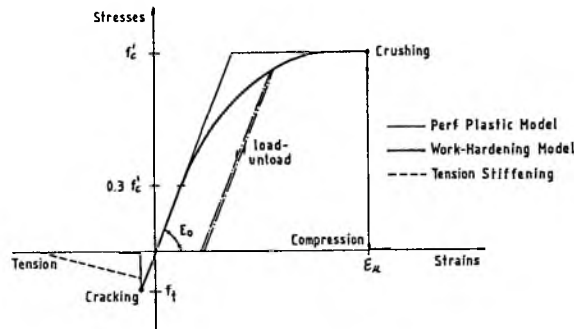


Fig. 1. One-dimensional representation of the constitutive model of concrete.

Crushing or compressive type of fracture is assumed to occur when the effective total strain reaches the limit value, which is usually taken as the maximum compressive strain in a uniaxial compression test. Once crushing has occurred, the concrete is assumed to lose all its characteristics of stiffness at the point under consideration. Therefore, the corresponding elasticity matrix  $D$  is taken as a null matrix and the vector of total stresses is reduced to zero.

**Tensile Behavior of Concrete.** The relative weakness of concrete in tension and the resulting cracking is a fundamental factor affecting nonlinear behavior of reinforced concrete plates and shells. It is assumed that when concrete is subjected to tensile stress it behaves like an elastic-brittle material. The formation of cracks is a brittle process and the concrete strength in the tension-loading direction abruptly goes down to zero after such cracks have formed (Fig. 2).

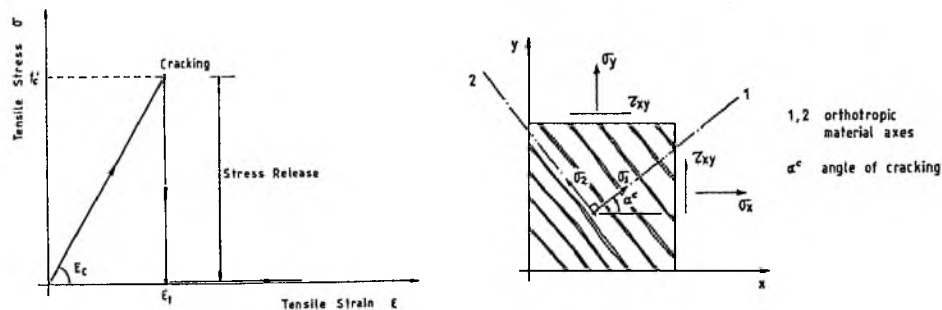


Fig. 2. Behavior of concrete under traction, smeared crack model, and the corresponding material axes for concrete cracked in one direction.

**Smeared Crack Model.** In our analysis, we are not interested in the tensile strength of concrete, but in the influence of the cracked zones on the concrete structural behavior. A simplified averaging procedure for finite element representation is adopted based on smeared cracked concrete, which assumes that cracks are distributed across the region of the finite element [11, 12].

In this model, cracked concrete is supposed to remain a continuum and the material properties are then modified to account for the damage induced in the material. After the first crack has occurred, the concrete becomes orthotropic with the material axes oriented along the directions of cracking (Fig. 2).

The response of concrete under tensile stresses is assumed to be linear-elastic until the fracture surface is reached. This tensile type of fracture or cracking is governed by the maximum tensile stress criterion (tension cut-off). Cracks are assumed to form in planes perpendicular to the direction of the maximum tensile stress, as soon as this stress reaches the specified concrete tensile strength  $f'_t$ . A sudden and total release of the normal stress in the affected direction, or its gradual relaxation according to a tension-stiffening diagram is adopted after cracking has occurred. The elasticity modulus and Poisson's ratio are reduced to zero in the direction perpendicular to the cracked plane, and a reduced shear modulus is employed [11, 12]. Before cracking, concrete is assumed to be an isotropic material with the following stress-strain relationship:

$$\begin{Bmatrix} \sigma_x \\ \sigma_y \\ \tau_{xy} \\ \tau_{xz} \\ \tau_{yz} \end{Bmatrix} = \begin{bmatrix} \frac{E}{1-\nu^2} & \frac{\nu E}{1-\nu^2} & 0 & 0 & 0 \\ \frac{\nu E}{1-\nu^2} & \frac{E}{1-\nu^2} & 0 & 0 & 0 \\ 0 & 0 & G & 0 & 0 \\ 0 & 0 & 0 & \alpha G & 0 \\ 0 & 0 & 0 & 0 & \alpha G \end{bmatrix} \begin{Bmatrix} \varepsilon_x \\ \varepsilon_y \\ \gamma_{xy} \\ \gamma_{xz} \\ \gamma_{yz} \end{Bmatrix}. \quad (4)$$

Here  $x$  and  $y$  are the axes in the plane of the structure,  $E$  is the elasticity modulus,  $\nu$  is Poisson's ratio,  $G$  is the shear modulus,  $G = E/2(1 + \nu)$ , and  $\alpha$  is the shear correction factor ( $\alpha = 5/6$ ). Taking 1 and 2 as the two principal stress directions in the plane of the structure, the stress-strain relationship for concrete cracked in the 1-direction (crack plane normal to 1-direction) is

$$\begin{Bmatrix} \sigma_1 \\ \sigma_2 \\ \tau_{12} \\ \tau_{13} \\ \tau_{23} \end{Bmatrix} = \begin{bmatrix} 0 & 0 & 0 & 0 & 0 \\ 0 & E & 0 & 0 & 0 \\ 0 & 0 & G_{12}^c & 0 & 0 \\ 0 & 0 & 0 & G_{13}^c & 0 \\ 0 & 0 & 0 & 0 & \alpha G \end{bmatrix} \begin{Bmatrix} \varepsilon_1 \\ \varepsilon_2 \\ \gamma_{12} \\ \gamma_{13} \\ \gamma_{23} \end{Bmatrix}, \quad (5)$$

where  $G^c$  is the reduced shear modulus of cracked concrete [11, 12]. When the tensile stress in the 2-direction reaches the value  $f'_t$ , the second cracked plane perpendicular to the first one is assumed to form and the stress-strain relationship for concrete cracked in two directions becomes

$$\begin{Bmatrix} \sigma_1 \\ \sigma_2 \\ \tau_{12} \\ \tau_{13} \\ \tau_{23} \end{Bmatrix} = \begin{bmatrix} 0 & 0 & 0 & 0 & 0 \\ 0 & 0 & 0 & 0 & 0 \\ 0 & 0 & \frac{G_{12}^c}{2} & 0 & 0 \\ 0 & 0 & 0 & G_{13}^c & 0 \\ 0 & 0 & 0 & 0 & G_{23}^c \end{bmatrix} \begin{Bmatrix} \varepsilon_1 \\ \varepsilon_2 \\ \gamma_{12} \\ \gamma_{13} \\ \gamma_{23} \end{Bmatrix}, \quad (6)$$

The cracked concrete is anisotropic and these relations must be transformed to the reference axes, similarly to composite materials.

**Behavior of Steel Re-Bars in Tension and Compression.** Steel reinforcing bars used in reinforced concrete structures are usually round with protrusions (ribs or lugs). These protrusions are responsible for better bond characteristics between the reinforcing bars and the surrounding concrete. Steel bars have elastoplastic behavior defined by its yield strength with a typical elasticity modulus of 210 GPa. A yield plateau, whose extension depends on the class of steel, is followed by strain-hardening behavior up to failure. In this model, the reinforcing bars are modeled as steel layers of equivalent thickness. Each steel layer exhibits a uniaxial response, having strength and stiffness characteristics in the bar direction only. The elastoplastic behavior is treated incrementally as a one-dimensional problem.

**Behavior of Composite Strips in Tension and Compression.** Composite strips made usually from carbon/epoxy materials are bonded together at the tension face of concrete, in order to improve the tension characteristics of concrete. These strips are typically made from unidirectional composites with unidirectional properties. They are considered as elastic-brittle materials, with no yield strength, having only ultimate strength. When the stresses in these layers reach a specified ultimate tensile strength of the composite material, the material is assumed to lose all its stiffness and strength, as in a typical concrete layer. The material characteristics are orthotropic and are defined as in Eqs. (10)–(12). Typical composites made from unidirectional epoxy/carbon materials have a modulus of 180 GPa and ultimate stress of about 1500 MPa.

**Shear-Deformation Theories.** *First Order Shear-Deformation Theories.* Yang, Norris, and Stavsky [9] and Stavsky [10] have developed a theory of deformation based on the work of Mindlin [15] and Reissner [16] for isotropic plates. The displacement field is obtained as

$$\begin{cases} u(x, y, z) = u_0(x, y) + z\theta_x(x, y), \\ v(x, y, z) = v_0(x, y) + z\theta_y(x, y), \\ w(x, y, z) = w_0(x, y), \end{cases} \quad (7)$$

where  $u$ ,  $v$ , and  $w$  are the  $x$ ,  $y$ , and  $z$  displacements. The  $u_0$ ,  $v_0$ , and  $w_0$  are the midplane displacements, and  $\theta_x$  and  $\theta_y$  are the rotations of the normal. Stress-strain relations can be expressed as

$$\begin{bmatrix} \varepsilon_x \\ \varepsilon_y \\ \gamma_{xy} \end{bmatrix} = \begin{bmatrix} \varepsilon_x^0 \\ \varepsilon_y^0 \\ \gamma_{xy}^0 \end{bmatrix} + z \begin{bmatrix} \kappa_x \\ \kappa_y \\ \kappa_{xy} \end{bmatrix} = \hat{\varepsilon}^0 + z\hat{\kappa}, \quad (8)$$

$$\begin{bmatrix} \gamma_{xz} \\ \gamma_{yz} \end{bmatrix} = \begin{bmatrix} w_{,x} + \theta_x \\ w_{,y} + \theta_y \end{bmatrix}, \quad (9)$$

where

$$\begin{aligned} \varepsilon_x^0 &= u_{0,x}, & \varepsilon_y^0 &= v_{0,y}, & \gamma_{xy}^0 &= v_{0,x} + u_{0,y}, \\ \kappa_x &= \theta_{x,x}, & \kappa_y &= \theta_{y,y}, & \kappa_{xy} &= \theta_{x,y} + \theta_{y,x} \end{aligned} \quad (10)$$

are the membrane deformations and plane curvatures, respectively.

In each layer  $k$  of the laminate, the stress-strain relations are obtained as

$$\begin{bmatrix} \sigma_{11} \\ \sigma_{22} \\ \tau_{12} \end{bmatrix}_k = \begin{bmatrix} c_{11} & c_{12} & c_{13} \\ c_{12} & c_{22} & c_{23} \\ c_{13} & c_{23} & c_{33} \end{bmatrix}_k \begin{bmatrix} \varepsilon_{11} \\ \varepsilon_{22} \\ \gamma_{12} \end{bmatrix}_k, \quad \begin{bmatrix} \tau_{13} \\ \tau_{23} \end{bmatrix}_k = \begin{bmatrix} c_{44} & c_{45} \\ c_{45} & c_{55} \end{bmatrix}_k \begin{bmatrix} \gamma_{13} \\ \gamma_{23} \end{bmatrix}_k, \quad (11)$$

where  $c_{ij}$  are elastic coefficients and  $\{1, 2, 3\}$  are the principal material directions for each layer. This theory is simple but introduces a shear correction coefficient [11, 13] that affects only the shear terms.

*Higher Order Shear-Deformation Theories.* The higher order shear-deformation theories avoid the use of the shear correction factors by a better representation of the “normal” warping. Various theories were proposed in the literature [7–10]. The model proposed in this paper has the following displacement field:

$$\hat{u} = \hat{u}^0 + z\hat{\theta} + z^3\hat{\theta}^*, \quad (12)$$

where  $\hat{\theta}^*$  represents the higher order rotations.

In these theories, the transverse displacement is constant throughout the plate or shell thickness. This theory has the advantage that no shear-correction factors are needed.

In sandwich laminates, these theories present some difficulties. The layer-wise theory proposed allows for a better deformation analysis in the laminate.

**Finite Element Implementation.** The theories presented so far were implemented in a degenerated shell element [4–6, 17]. Two main coordinate systems are used in the element [17]: the global Cartesian coordinate system  $(x, y, z)$ , in relation to which the nodal coordinates and displacements are defined, and the curvilinear coordinate system  $(\xi, \eta, \zeta)$ , where the shape functions  $N_k$  are expressed. The midsurface of the element is defined by the  $\xi$  and  $\eta$  coordinates. In the Ahmad shell element,  $\zeta$  is a linear coordinate in the thickness direction and is only approximately normal to the shell midsurface. Ahmad degenerated a three-dimensional brick element to a curved shell element, which has nodes at the midsurface [17]. In addition to the coordinate systems mentioned above, this element defines two more sets as can be seen in Fig. 4. A nodal Cartesian coordinates system  $(v_{1k}, v_{2k}, v_{3k})$  is associated with each nodal point of the element and has its origin at the midsurface. The unit vector  $\bar{\mathbf{v}}_{3k}$  constructed from the nodal coordinates of the top,  $\mathbf{x}_k^{top}$ , and bottom,  $\mathbf{x}_k^{bot}$ , surfaces at the node  $k$ , determines the ‘normal’ direction  $v_{3k}$ , which is not necessarily perpendicular to the reference surface. The unit vectors  $\bar{\mathbf{v}}_{1k}$  (direction  $v_{1k}$ ) and

$\vec{v}_{2k}$  (direction  $v_{2k}$ ) define the nodal rotations  $\beta_{2k}$  and  $\beta_{1k}$ , respectively, of the ‘normal’ mentioned above. The local Cartesian coordinate system  $(x', y', z')$  is used to define the local stresses and strains at the sampling points wherein they must be calculated. The vector direction  $\mathbf{z}'$  is taken to be orthogonal to the surface  $\zeta = \text{const}$ , the direction  $\mathbf{x}'$  is defined similarly to that of  $\vec{v}_{1k}$  and, finally,  $\mathbf{y}'$  is obtained by the cross product of  $\mathbf{z}'$  and  $\mathbf{x}'$ . This coordinate system varies along the thickness of the element and it is useful to define the direction cosine matrix  $\hat{\theta}$ , which relates the transformations between the local and global coordinate systems; this matrix is defined by

$$\hat{\theta} = [\bar{\mathbf{x}}' \quad \bar{\mathbf{y}}' \quad \bar{\mathbf{z}}'], \quad (13)$$

where  $\bar{\mathbf{x}}'$ ,  $\bar{\mathbf{y}}'$ , and  $\bar{\mathbf{z}}'$  are unit vectors along the directions  $\mathbf{x}'$ ,  $\mathbf{y}'$ , and  $\mathbf{z}'$ , respectively.

The coordinates  $\mathbf{x}$  of a point within the element are obtained as

$$\mathbf{x} = [x, y, z]^T = \sum_{k=1}^n N_k(\xi, \eta) [\mathbf{x}_k^{mid} + h_k \zeta / 2 \vec{v}_{3k}]. \quad (14)$$

The displacements for the first-order shear deformation are obtained as

$$\hat{\mathbf{u}} = \sum_{k=1}^n \hat{N}_k \hat{\mathbf{u}}_k^{mid} + \sum_{k=1}^n \hat{N}_k \zeta \frac{h_k}{2} [V_{1k}, -V_{2k}] \begin{Bmatrix} \beta_{1k} \\ \beta_{2k} \end{Bmatrix} \quad (15)$$

whereas for the third-order theory they are obtained as

$$\begin{aligned} \hat{\mathbf{u}} = & \sum_{k=1}^n \hat{N}_k \hat{\mathbf{u}}_k^{mid} + \sum_{k=1}^n \hat{N}_k \zeta \frac{h_k}{2} [V_{1k}, -V_{2k}] \begin{Bmatrix} \beta_{1k} \\ \beta_{2k} \end{Bmatrix} + \\ & + \sum_{k=1}^n \hat{N}_k \left( \zeta \frac{h_k}{2} \right)^3 [V_{1k}, -V_{2k}] \begin{Bmatrix} \beta_{1k}^* \\ \beta_{2k}^* \end{Bmatrix} \end{aligned} \quad (16)$$

for other layers. In (16),  $\beta_{1k}^*$  and  $\beta_{2k}^*$  represent the higher-order rotations. The parameter  $n$  is the number of nodes per element,  $h_k$  is the shell thickness at the node  $k$ , i.e., the respective ‘normal’ length,  $\mathbf{u}_k^{mid}$  and  $\mathbf{x}_k^{mid}$  are, respectively, the displacements and the global coordinates at the midsurface, and  $N_k(\xi, \eta)$  are the element shape functions.

**Numerical Example.** A single span beam tested by Bresler and Scordelis [18] is selected for analysis. The beam is simply supported, subjected to a concentrated load at midspan and has a shear span to effective depth ratio of about 7. The type of failure experimentally observed for the beam was brittle

fracture due to flexure-compression. The beam failed by crushing of the concrete compression zone near midspan. This is a good example to compare the model developed for compression concrete, namely, the perfect plastic and the hardening plastic models. In the experiment, the beams were first loaded to about 30 percent of the ultimate load in two or three increments and then the load was removed. The load was reapplied in small increments until failure occurred. The available experimental curves were obtained from the deflections recorded during the final cycle of loading from zero to the ultimate value. In the analysis, the load is applied incrementally in one cycle from zero to the ultimate.

The loading conditions and the span are illustrated in Fig. 3. The stirrups are not considered in the analysis. Brittle fracture of concrete by crushing before yielding of the steel is expected, therefore, the post-yield diagram of the main reinforcement is not of great importance in this study.

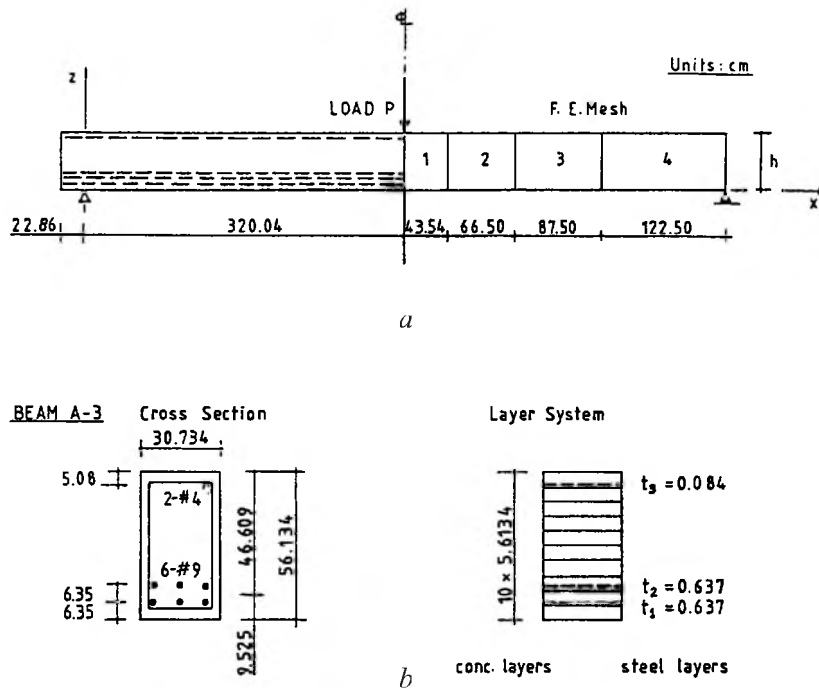


Fig. 3. A simply supported RC beam. Geometry, mesh, and layered structure.

Taking advantage of the symmetry, we analyzed only one half of the span. Four finite elements are used to refine the mesh near the center, where larger nonlinear effects are expected (Fig. 2). Selective integration is employed to obtain a better representation of the material behavior particularly near the applied load.

Ten concrete layers of equal thickness and three smeared steel layers are used to discretize the beam through the thickness. The smeared thickness of each layer is specified in Fig. 2.

Midspan deflections versus total load are plotted in Fig. 4. The numerical solutions performed with the present model, either by using the perfect plastic (PP) or the hardening plastic (HP) approach for concrete in compression are compared with the experimental curve. Excellent agreement is shown between the

experimental and the hardening plastic results. The slight discrepancy for lower load range is attributed to the previously mentioned unloading and reloading experimental cycle. The slightly higher collapse load (2.6%) may be due to the coarse thickness considered for the concrete top layer. One of the main steel reinforcement layers (the bottom one) starts to yield at  $P = 470$  kN, therefore, the assumed steel post-yield diagram may have some influence on the ultimate load. The results obtained with the perfectly plastic model show a stiffer response for higher loads and a greater (nonconservative) collapse load.

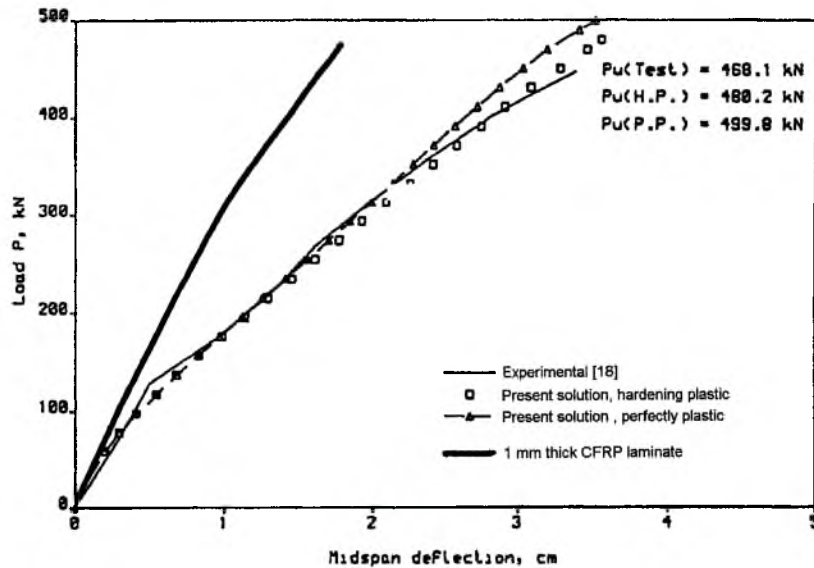


Fig. 4. A simply supported RC beam. Comparison of experimental and numerical results.

The third-order shear-deformation approach seems to be efficient in the analysis of such structures.

Figure 4 also presents a load-displacement curve for an RC beam with an external 1 mm thick CFRP laminate in the tension side (bottom face). The overall load-displacement behavior is much stiffer than for a RC beam without any laminate reinforcement.

**Conclusions.** The material and geometrical nonlinearities for reinforced concrete strengthened with fiber-reinforced plastics were investigated. The material model for concrete was based on a dual approach for compressive and tensile behavior, with degradation of properties due to cracking and crushing. Steel reinforcements are considered as unidimensional elastoplastic solids, while composite reinforcements are considered as elastobrittle solids. A third-order approach for the reinforcement of concrete shells with external composite laminates was presented. A perfect plastic and a strain-hardening plasticity approach were used to model the compressive behavior of concrete. A dual criterion for yielding and crushing in terms of stresses and strains was considered with a tension cut-off representation. The material behavior of unidirectional composites is linear elastic/brittle. The concrete allows for elastoplastic-brittle behavior. A simply supported concrete beam reinforced with composite strips was

analyzed. The effects of the reinforcement on concrete, comparison of composite strengthening by steel re-bars, and the use of the third-order theory for their description were discussed. A good agreement between the experimental and numerical results was found for RC beams. When strengthened with CFRP sheets, the behavior of the beam becomes stiffer as expected. The cracking by tension is delayed to higher loads. The overall behavior is much more stiff. However, this model does not take into account the influence of the adhesive layer, which may change the load–displacement behavior.

**Acknowledgements.** The support of Fundação para a Ciência e Tecnologia under project POCTI/35955/EME/2000 is gratefully acknowledged.

## Резюме

Запропоновано теорію зсувної деформації третього порядку для опису напружено-деформованого стану армованих зовнішніми композитними ламінатами бетонних оболонок. Армовані бетонні конструкції – головні компоненти в галузі будівництва. Корозія сталевих балок, що використовуються для армування залізобетонних конструкцій, – дуже актуальна проблема, яка посилюється за рахунок пористості бетону. Адекватним вирішенням проблеми зміцнення і модифікації ослаблених конструкцій є використання зовнішніх композитних ламінатів, котрі закріплюються на зовнішніх поверхнях бетонних конструкцій. Деформування такого роду конструкцій характеризується значною нелінійністю. Для розробки нелінійних геометричних моделей та моделей матеріалу використовуються числові методи, зокрема метод скінчених елементів. Для аналізу композитних ламінатів часто використовують зсувні деформації високого порядку. Запропонована теорія є альтернативою теорії першого порядку, яку запропонував раніше Феррейра зі співавторами. Теорія опробована при розрахунку елемента оболонки, структура якого дозволяє відтворити пошарову дискретизацію ламінатних матеріалів. Для моделювання деформування бетону при стиску використовувалися підходи ідеально пластичної та пластично-зміцнюваної поведінки матеріалу. Розглянуто двоїстий критерій текучості і руйнування матеріалу з точки зору напружень та деформацій, який використовується в поєднанні з представленням деформаційної кривої при розтязі у вигляді ломаної лінії з горизонтальною ділянкою, що відповідає початку пластичної текучості. Односпрямовані композитні смуги характеризуються лінійно-пружною (крихкою) поведінкою. Виконано скінченноелементний розрахунок напружено-деформованого стану армованої композитними смугами бетонної балки, яку піддавали триточковому згину. Описано спостережувані ефекти армування, результати використання теорії третього порядку і проведено порівняльний аналіз зміцнення бетонної конструкції композитними смугами і сталюю арматурою.

1. O. C. Zienkiewicz, *The Finite Element Method*, McGraw-Hill (1991).
2. M. A. Crisfield, *Nonlinear Finite Element Analysis of Solids and Structures*, John Wiley & Sons (1991).

3. K. J. Bathe, *Finite Element Procedures in Engineering Analysis*, Prentice Hall, Englewood Cliffs (1982).
4. U. Meyer and A. Winistorfer, "Retrofitting of structures through external bonding of CFRP sheets," in: Proc. 2nd Int. RILEM Symp. FRPRCS-2, E&FN Spon, London (1995).
5. L. Juvandes, J. A. Figueiras, and A. T. Marques, "Performance of concrete beams strengthened with CFRP laminates," in: H. Saadatmanesh and M. R. Eshani (Eds.), *Fiber Composites in Infrastructure* (Proc. Second Inter. Conf. on *Composites in Infrastructure*), Tucson (1998).
6. A. Nanni, F. Focacci, and C. A. Cobb, "Proposed procedure for the design of RC flexural members strengthened with FRP sheets," in: H. Saadatmanesh and M. R. Eshani (Eds.), *Fiber Composites in Infrastructure* (Proc. Second Inter. Conf. on *Composites in Infrastructure*), Tucson (1998).
7. J. N. Reddy, "A simple higher-order theory for laminated composite plates," *J. Appl. Mech.*, **51**, 745–751 (1984).
8. T. Kant and D. R. J. Owen, "A refined higher-order  $C^\circ$  plate bending element," *Comp. Struct.*, **15**, 177–183 (1982).
9. P. C. Yang, C. H. Norris, and Y. Stavsky, "Elastic wave propagation in heterogeneous plates," *Int. J. Sol. Struct.*, **2**, 665–684 (1966).
10. Y. Stavsky, "Bending and stretching of laminated aerolotropic elastic plates," *J. Eng. Mech. Div.*, **87**, 31–56 (1961).
11. A. J. M. Ferreira, *Numerical Models for the Analysis of Composite and Sandwich Laminated Structures* [in Portuguese], Ph. D. Thesis, Faculdade de Engenharia da Universidade do Porto, Porto (1997).
12. D. R. J. Owen and J. A. Figueiras, "Ultimate load analysis of reinforced concrete plates and shells," in: E Hinton and D. R. J. Owen (Eds.), *Finite Element Software for Plates and Shells*, Pineridge Press (1984).
13. J. A. Figueiras, *Ultimate Load Analysis of Anisotropic and Reinforced Concrete Plates and Shells*, Ph. D. Thesis, University College of Swansea (1983).
14. H. Kupfler, K. H. Hilsdorf, and H. Rush, "Behavior of concrete under biaxial stresses," in: *Proc. Amer. Concrete Institute*, **66**, No. 8, 656–666 (1969).
15. R. D. Mindlin, "Influence of rotary inertia and shear on flexural motions of isotropic elastic plates," *J. Appl. Mech.*, **18** (1), *Trans. ASME*, **73**, 31–38 (1951).
16. E. Reissner, "The effects of transverse shear deformation on the bending of elastic-plates," *J. Appl. Mech.*, **12** (2), *Trans. ASME*, **67**, 69–77 (1945).
17. S. Ahmad, B. Irons, B. M. Zienkiewicz, and O. C. Zienkiewicz, "Analysis of thick and thin shell structures by curved finite elements," *Int. J. Num. Meth. Eng.*, **2**, 419–451 (1970).
18. R. Bresler and A. C. Scordelis, "Shear strength of reinforced concrete beams," *ACI Journal*, Proc., **60**, No. 1, 51–73 (1963).

Received 05. 09. 2002